Roof Crush Resistance and Rollover Strength of a Paratransit Bus

Cezary Bojanowski [1]
Bronislaw Gepner[2a]
Leslaw Kwasniewski[3]
Christopher Rawl[2b]
Jerry Wekezer[2c]

1) *Transportation Research and Analysis Computing Center,*
Energy Systems Division, Argonne National Laboratory
9700 S. Cass Avenue, Argonne, IL 60439-4828, USA
cbojanowski@anl.gov

2) *FAMU-FSU College of Engineering,*
Department of Civil and Environmental Engineering
2525 Pottsdamer Street, Tallahassee, FL 32310-6046, USA
a) bgepner@fsu.edu   b) rawlch@eng.fsu.edu   c) wekezer@eng.fsu.edu

3) *Warsaw University of Technology, Faculty of Civil Engineering*
Al. Armii Ludowej 16, 00-637 Warsaw, Poland
l.kwasniewski@il.pw.edu.pl

Abstract

Paratransit buses constitute a special group of vehicles in the US due to their smaller size, two-step assembly process, and their use for complementary services to the regular scheduled transit routes. Due to their uniqueness these buses lack national crashworthiness standards specifically dedicated to the paratransit fleet. Several states in the US adopted the quasi-static symmetric roof loading procedure according to the standard FMVSS 220 for testing the integrity of the paratransit buses. However, as many researchers point out, the dynamic rollover test according to UN-ECE Regulation 66 (ECE-R66), which was approved by more than forty countries in the world, (excluding the US), may provide more realistic assessment of the bus strength.

This paper provides comparison of the numerically assessed strength of the paratransit bus according to the two standards in explicit FE simulations using LS-DYNA®/MPP. The FE model used in this study was previously validated through comparison of its simulated behavior with response of the bus in the full scale rollover test conducted at the Florida Department of Transportation testing facility (Tallahassee, FL, USA, 2010).

The results show that the final assessment of the bus crashworthiness from both procedures can be divergent. Although the tested bus passes the quasi-static FMVSS 220 test, the same bus fails the dynamic rollover procedure of ECE-R66 test. While the paratransit fleet is outnumbered by the regular transit buses, and experimental testing of the buses seems to be prohibitively expensive to local manufacturers, the FE simulations provide viable insight into the bus strength.

Keywords: *Rollover, UN-ECE Regulation 66 (ECE-R66), Roof crush, FMVSS 220, crashworthiness*

1. Introduction

Paratransit buses form a special group of vehicles in the US. In comparison to the transit buses they are considerably smaller and are used for different purposes. They complement services provided to the regular transit routes and are usually equipped with wheelchair lifts and floor mounts for wheelchairs tiedown systems. Paratransit buses are built in a two-step process: first - the chassis from a bigger automotive company is adopted and then a passenger compartment is constructed on it at a smaller, local assembly line. It makes this group of vehicles very unique in the US in the sense that they are not regulated by any national crashworthiness standard. The number of severe accidents with paratransit buses does not justify supporting an extensive research on them. However, problems with their strength were identified and should not be ignored.

Several states in the US try to overcome that loophole requiring paratransit buses to comply with the Federal Motor Vehicle Safety Standard FMVSS 220 standard "School bus rollover protection". It requires a quasi-static application of a loading equal to 1.5 times of the unloaded vehicle weight (UVW) to assess the static response of the bus roof structure. The resistance of the roof structure is judged as satisfactory when: the downward vertical movement at any point on the application plate does not exceed 5⅛ inches (130 mm) and each emergency exit of the vehicle can be opened during full application of the force and after the release of the force.

Many researchers point out that such quasi-static tests with symmetric roof loading poorly represent the sequential dynamic load (in particular it's varying value, direction, and intensity) observed during actual bus rollovers. Nevertheless, they may provide greater repeatability of results than foreign dynamic test procedures like the European Union (EU) directives and the United Nations (UN) regulations - UN ECE Regulation 66 (ECE R66) *(1)*. ECE-R66 refers to integrity of a bus structure in a dynamic rollover test.

Research and bus inspections conducted by the Florida DOT shows that paratransit buses usually have no problems with passing FMVSS 220 standard testing procedure. The reason behind it is a strong roof structures designed to withstand prescribed vertical load during the test. However, recently conducted experimental testing reveals that the same buses may fail the ECE-R66 procedure. Thus, whether or not the bus is approved for the use depends on the testing procedure we choose.

This paper shows results of two sets of LS-DYNA simulations for a selected model of paratransit bus using FMVSS 220 and ECE-R66 testing procedures. The FE model used in this study was previously validated through comparison of its simulated behavior with response of the bus in the full scale rollover test conducted at Florida Department of Transportation testing facility (Tallahassee, FL, USA, 2010) *(2)*. A sensitivity analysis using LS-OPT was performed to identify most crucial elements of the bus structure for the response of the bus in the two tests.

2. Finite Element Model of the Bus

The original FE model of the bus was developed in the two separate stages *(3)*. First, a model of a cutaway chassis was extracted from a public domain Ford Econoline Van FE model, developed

by the National Crash Analysis Center (NCAC) at George Washington University *(4)*. The FE model was modified to match specifications of the chassis used for the given paratransit bus – from the van E-150 to the heavy duty E-450. Major changes have been made to the main chassis beams and suspension elements. During the second stage of FE model development, the 3D geometry and FE models of separate bus body walls (side walls, back wall, roof and floor) were created from CAD drawings supplied by the bus manufacturer. Finally the bus body cage was assembled with the chassis using LS-PrePost.

Florida Department of Transportation is acquiring decommissioned paratransit buses for experimental testing and FE models validation. The recently acquired buses were similar to the FE model described in the paper. The paratransit buses are custom made and for each case the structure may be slightly different although the buses have the same make and model. Modifications had to be done to the FE model in order to be able to compare experimental and computational results. Also the mesh density was nearly doubled in the new model. The original bus model, containing ~538,000 finite elements, has been expanded to almost 925,000 finite elements. The major structural components had minimum four shell elements across their width. Fully integrated shells (ELFOR 16) were used in the whole model. The statistics of the final FE model are shown in Table 1. The full scale paratransit bus and its model are shown in Figure 1.

Table 1: Statistics of developed paratransit bus FE model

	Chassis model	**Bus body**	**Whole model**
# of elements	189,079	735,407	924,486
# of nodes	204,998	658,028	773,026
# of parts	295	64	359
# of 1-D elements	2	0	2
# of 2-D elements	173,401	735,407	908,808
# of 3-D elements	15,676	0	15,676

Figure 1: The bus selected for a rollover test (left) and its FE model (right)

A full rollover test was performed at Florida Department of Transportation testing facility in 2010. The results were used to validate the FE model of the bus *(2)*. Only the results of the simulations with the validated model are presented here.

3. Rollover Test Simulation According to ECE-R66 and FDOT Standard

In the rollover test procedure, a vehicle resting on a tilting platform (as shown in Figure 1) is quasi-statically rotated onto its weaker side. Depending on the attachments of the staircase and the door frame to the bus frame, it is usually the road side of the bus. When the center of gravity reaches the highest (critical) point, the rotation of the table is stopped. Further the gravity causes the bus to free-fall into a concrete ditch. The flooring in the ditch is located 800 mm beneath the tilt table horizontal position. LS-DYNA simulations involved simplified case where the bus was positioned in the configuration just before the impact with the ground. Initial velocities were applied to the structure of the bus to simulate appropriate conditions of the real test. Such approach saved computational time needed for each run.

The bus passes the rollover test if the residual space is not compromised during the tests *(1)*, *(5)*. The shape of the residual space is defined in Figure 2. The FDOT standard is based on the ECE-R66 but it contains several extensions. An additional quantity called Deformation Index (*DI*) was proposed in the FDOT standard for quantitative comparison of the results *(6)*. Consistently with the concept of the residual space - the *DI* is only providing information about the passenger compartment and not the driver's cabin. The *DI* is based on the assumption that during the rollover-induced impact, the angular deformations develop only in hypothetical plastic hinges located at vulnerable connections in the bus cross section. The rotations in these hinges are marked on the bus cross section as α_1 through α_6 in Figure 2a. The elastic deformations of the walls are neglected in this definition. Based on the geometry of the failure mode (Figure 2b), *DI* is defined as:

$$DI = \frac{l}{d} \cdot \tan(\Delta\alpha_1) + \frac{(h-l)}{d} \cdot \tan(\Delta\alpha_2) \tag{1}$$

For acceptable designs, *DI* is in the range $0 \leq DI < 1$. Once the deforming walls start to touch the residual space - the *DI* is equal to 1. When $DI \geq 1$, the structure of the wall intrudes into the residual space, and the bus fails the test.
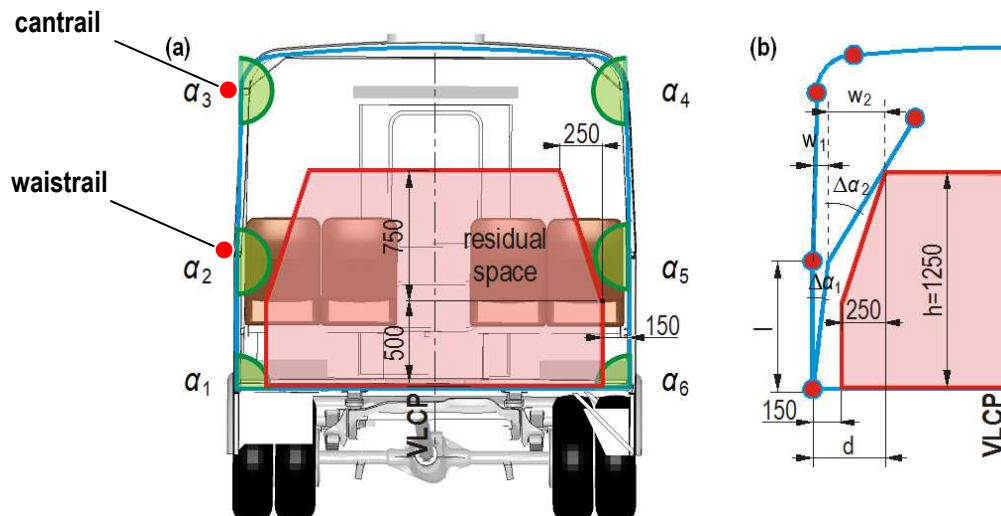

Figure 2: (a) Definition of the residual space (b) geometry of the failure mode (6)

The verified and validated FE model was used to simulate rollover test according to the ECE-R66. The deformations of the bus due to the impact are presented in Figure 3. The residual space is visibly penetrated by the wall pillars. Figure 4 shows history of the DI calculated using Equation 1. The bus significantly fails the test with DI reaching value of 2.1 at about 0.4 sec of simulation.
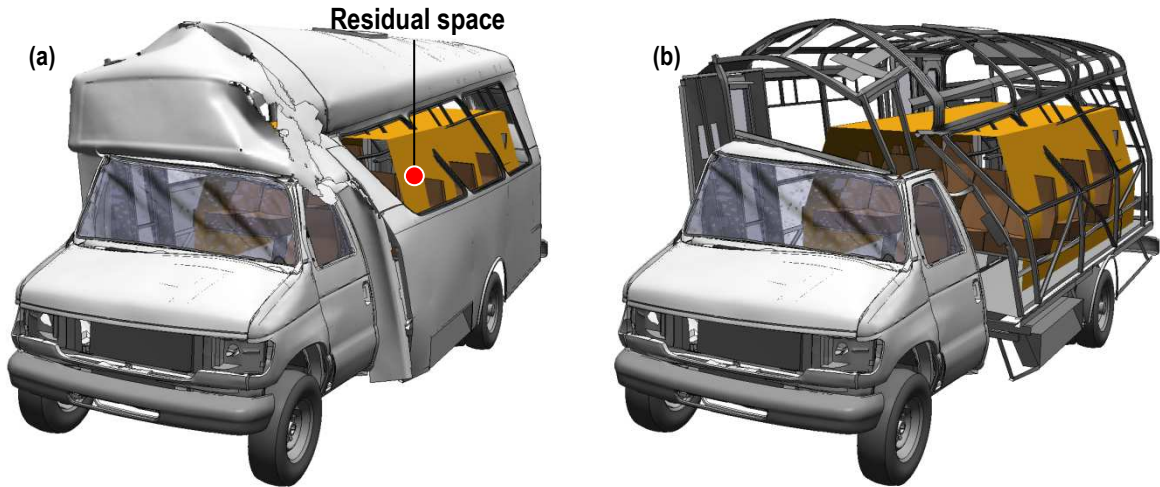

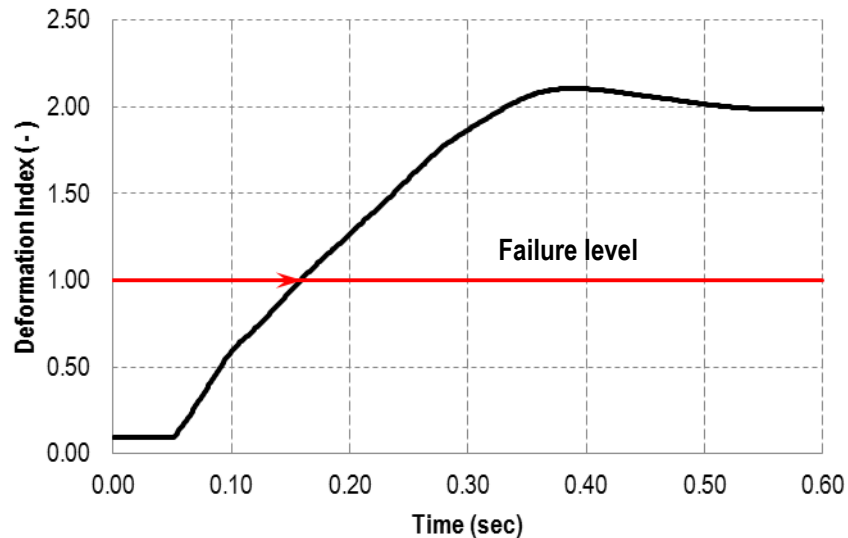*Figure 3: Residual space compromised by the bus structure. View of complete bus (a), view without skin (b)*

Figure 4: History of the Deformation Index measured in the rollover test simulation per FDOT standard

The bus is deformed in the torsional mode with rear part being considerably less deformed. As an outcome of the impact, the plastic deformations were developed at the front cap structure and at the waistrail beam. The cantrail beam was also deformed locally at the connections of the roof bows to the walls. Taking a closer look at the design of the front cap structure, one can find some obvious reasons of its weakness. The actual connections between the body and the driver's cabin are shown in Figures 5 and 6. The bus body is only connected by two flat pieces of steel on the road side of the bus. On the curb side, the driver's cabin is welded to the staircase in two spots (see Figure 6). The cap rests on the remainder of cabin roof and is connected with only

a few additional welds.

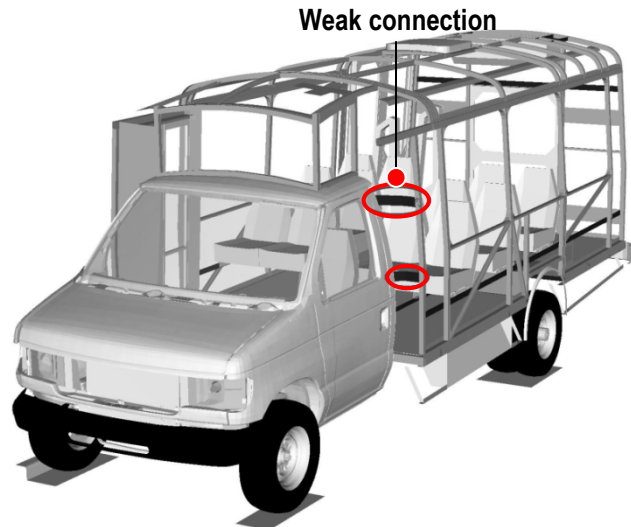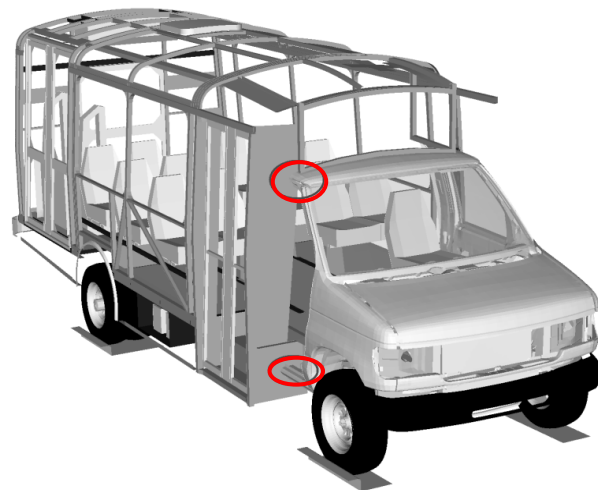*Figure 5: Connection of bus body to driver's cabin road side*

Figure 6: Connection of bus body to driver's cabin curb side

4. Roof Crush Resistance Test Simulation According to FMVSS 220 Standard

The same FE model, as used before for the ECE-R66 rollover simulation, was utilized to simulate the testing procedure of FMVSS 220 for roof crush resistance. An equivalent of 1.5 of Unloaded Vehicle Weight (UVW) is applied quasi-statically in this test procedure to the roof structure of the bus through a rigid plate. During the test, the resistance force and the displacement of the plate are recorded. This force should cause a roof deformation smaller than 130.2 mm (5.125 in) in order to pass the testing procedure. The bus chassis beams are directly supported so the deflection of the suspension is not taken into account in the test. Mass of the tested bus was equal to 4,636 kg (10,221 lb). Thus, the 1.5 of UVW was equivalent to the force of 68,219 N. The plate dimensions differ depending on the vehicle weight and in the FE model they followed the directions for the vehicle with GVWR of more than 4540 kg (10,000 lb).

The load was applied in two phases as specified in the FMVSS 220 standard. First, the pre-loading of 2,227 N (500 lbf) was applied to reduce slack in the system. In the computer simulation the loading was generated through the prescribed vertical displacement applied to the center of the plate. The plate was free to rotate about this point. The coefficient of friction for contact between the plate and roof structure was set as 0.15 (steel to steel) in AUTOMATIC_SURFACE_TO_SURFACE type of contact. In the LS-DYNA simulation the loading phase was shortened to 1 sec, and the mass of the application was reduced in order to eliminate inertial effects. Additional simulations were performed with lower loading rate. It turned out that the results were similar and the lower loading rate is not needed for further simulations.
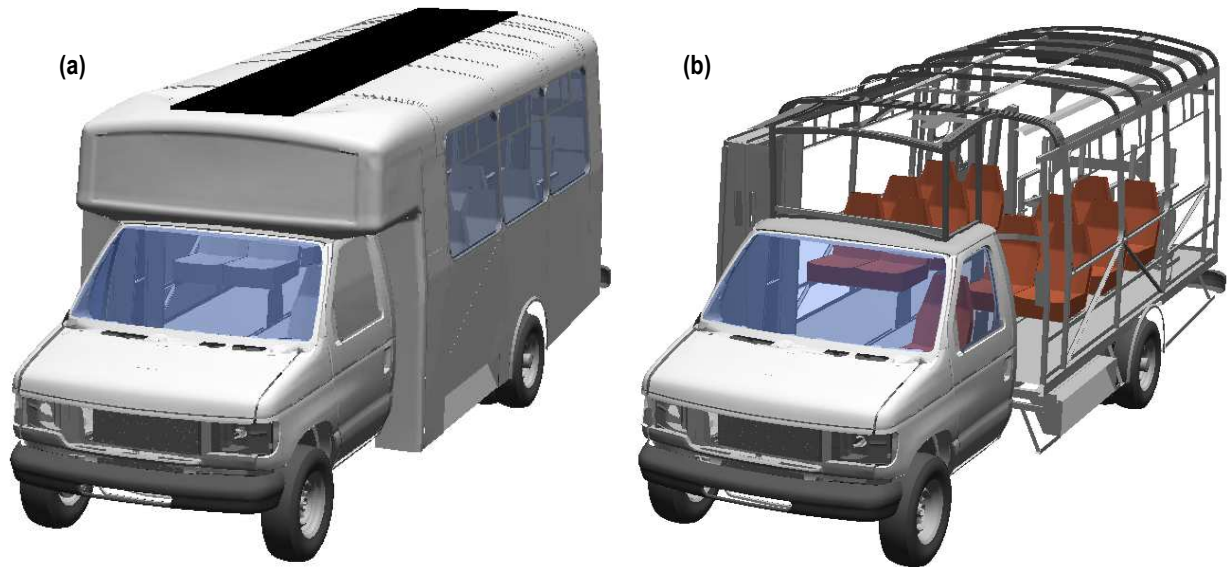

Figure 7: Residual space compromised by the bus structure. View of complete bus (a), view without skin (b)
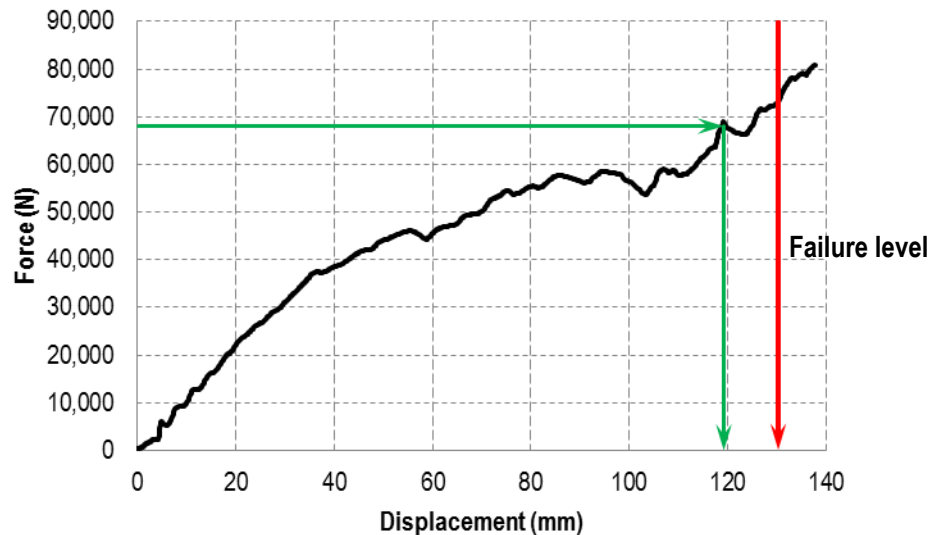

Figure 8: Time histories of displacements of the loading plate with zero displacement corresponding to the 2227 N (500 lbf) load

Figure 7 shows a view on the deformed structure of the bus. Figure 8 shows history plot of a force vs. loading plate displacement. The 1.5 UVW limit (equal to 68,219 N) was reached at 119 mm of penetration. Thus, unlike in the case of the ECE-R66, the bus considered passed the FMVSS 220 testing procedure.

5. Sensitivity Analysis

Bus manufacturers frequently strengthen up the roof structure to pass the FMVSS 220 testing procedures. The symmetric loading applied to the roof in the FMVSS 220, actually examines primarily the strength of the roof bows, without applying excessive loading on the rest of the structure. It is still not uncommon to see the design of paratransit bus where the open sections are used in the framing of the walls.

This chapter is aiming to analyze and rank significance of particular members of the structure in the response to the loading experienced in FMVSS 220 and ECE-R66 testing procedures for the selected bus. The analysis was carried out in LS-OPT 4.1 using Analysis Of Variance (ANOVA), and Global Sensitivity Analysis (GSA) with Sobol's approach *(7)*.

The ANOVA is performed in LS-OPT based on linear response surface fit to the obtained discrete results. The true continuous response $y(x)$ is approximated by the first order polynomial $f(x)$, defined as:

$$f(x) = \sum_{j=1}^{L} b_j \phi_j(x) \tag{2}$$

where:

$L-$ is the size of basis functions' vector ($\phi_j = [1, x_1, ..., x_n]^T$). The coefficients in the vector $\boldsymbol{b}$ are determined through minimization of the sum of the square errors computed by:

$$\sum_{i=1}^{P} \left\{ [y_i(x) - f_i(x)]^2 \right\} = \sum_{i=1}^{P} \left\{ \left[y_i(x) - \sum_{j=1}^{L} b_j \phi_j(x) \right]^2 \right\}, \tag{3}$$

where:

$f_i(x)-$ are responses predicted by metamodel,

$y_i(x)-$ are discrete responses calculated in LS-DYNA simulations,

$P-$ is the total number of sampling points.

The ANOVA plots in LS-OPT represent normalized b_j coefficients (see Equation 2) with their confidence intervals. The $100(1-\alpha)\%$ confidence intervals for the coefficients $b_j, j = 0,1,...,L$ are defined through *(8)*:

$$\beta_j \in \left[b_j - \frac{\Delta b_j(\alpha)}{2}, b_j + \frac{\Delta b_j(\alpha)}{2} \right] \tag{4}$$

For the cases, where the interaction parameters play significant role in approximating the response, application of Sobol's Indices may be more suitable. This approach uses a unique decomposition of a function into summands with increasing dimensions as *(9)*:

$$f(x_1,...,x_n) = f_0 + \sum_{i=1}^{n} f_i(x_i) + \sum_{i=1}^{n} \sum_{j=i+1}^{n} f_{ij}(x_i, x_j) + ... + f_{1,2,...,n}(x_1,...,x_n)$$ (5)

where:

$f(x_1,..., x_n)$ – represents the analyzed model with *n* random variables.

Each random model response $f_k(x_1,..., x_n)$ is characterized by its variance D^k. This variance can be also decomposed into partial variances as:

$$D^k = \sum_{i=1}^{n} D_i^k + \sum_{i=1}^{n} \sum_{j=i+1}^{n} D_{ij}^k + ... + D_{1,2,...,n}^k$$ (6)

The Sobol's Indices are defined by:

$$S(i_1,..,i_s) = \frac{D_{i_1,...,i_s}^k}{D^k}$$ (7)

where:

$S_i = \dfrac{D_i}{D}$ – is the main effect of the parameter and,

S_{Ti} – is the total effect, which combines parameter's main effect and all the interactions involving that parameter.

Computation of components in Equation (5) involves a multi-dimensional integration. In practice only the main and total effects are computed using the approximate formulas based on the Monte Carlo integrations *(9)*.

Figure 9 shows the passenger compartment frame with ten numbered parts. Thicknesses of elements in these parts were used in the design of experiments (DOE) study as the design variables. The baseline values for them as well as assumed lower and upper bounds for the region of interest in the DOE are listed in Table 2. The metal sheet thickness is described by manufacturers by discrete gauges. The equivalent metric measurement of the gauge depends on the material from which the members are built. The gauge conversions to SI and US units are listed in APPENDIX A.
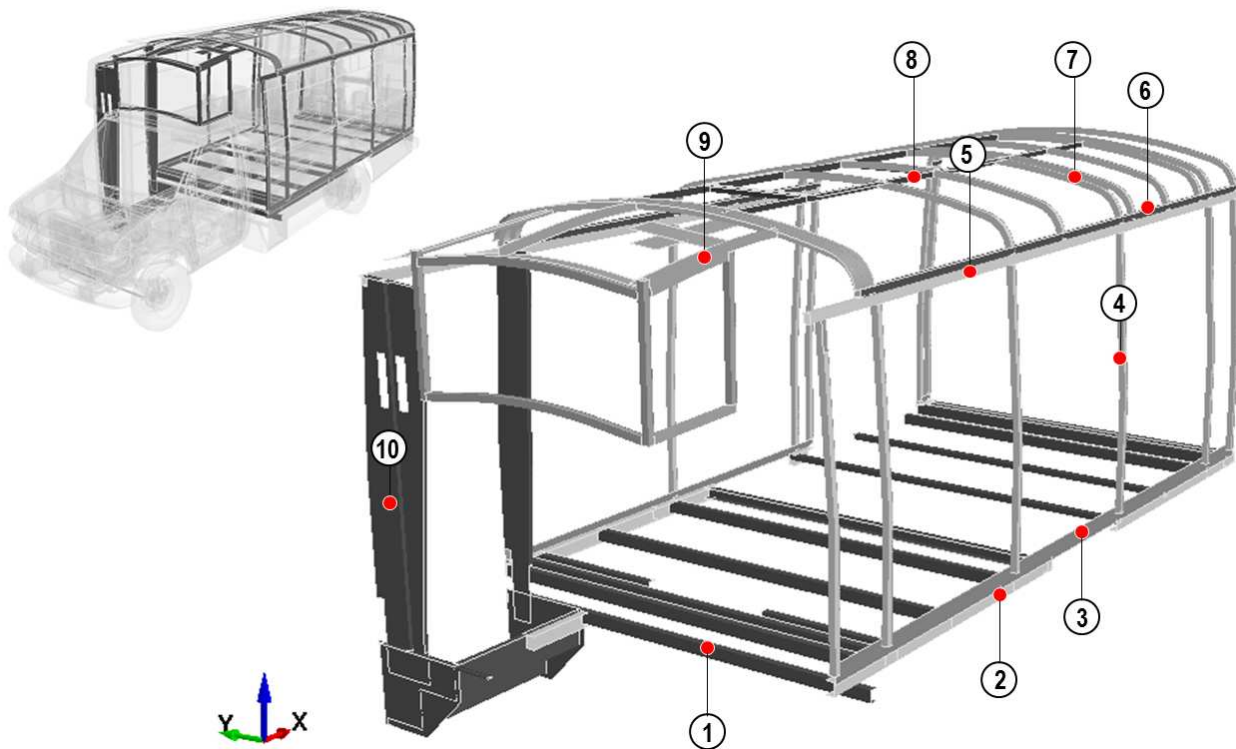
Figure 9: Location of the structural elements used in definition of design variables

Table 2: Variables used in the optimization process with assumed thickness range from 11 to 18 ga

	Variable	Symbol	Baseline Design (ga)
(1)	thickness of cross beams in the floor structure	*floor_cc*	11
(2)	thickness of longitudinal beams in the floor structure	*floor_cl*	16
(3)	thickness of S-shape connections in the wall structure	*floor_s*	16
(4)	thickness of square tubes in the wall structure	*wall_sq*	16
(5)	thickness of tubes at the cantrail location	*can_sq*	16
(6)	thickness of U-shapes at the cantrail location	*roof_u*	16
(7)	thickness of the roof bows	*roof_sq*	16
(8)	thickness of the longitudinal beams in the roof structure	*roof_mid*	16
(9)	thickness of the elements in the front cap structure	*cap_sq*	16
(10)	thickness of the staircase	*stairca*	16

The sensitivity was analyzed with respect to the Deformation Index for the case of ECE-R66 test. The *DI* response in LS-OPT was defined through Equation (1) based on nodal distances in the most vulnerable cross section of the bus. For the FMVSS 220 test sensitivity was studied with respect to the resistance force measured from the contact between the rigid plate and the bus roof structure.

The responses were approximated using Radial Basis Function Network. The design points were distributed using space filling algorithm. Fifty simulations per test were performed (total of 100 of simulations). Single precision LS-DYNA/MPP in version r5.0 was adopted for all runs. Six

compute nodes (48 CPUs) were used for each simulation. The calculation time for rollover test simulations was ~18 hours and ~25 hours for the roof crush test simulation respectively.

Figure 10 shows the sensitivity studies for Deformation Index in ECE-R66 test simulations. The most important element of the structure turned out to be the cantrail square beam (*can_sq*). The second most important was front cap structure (*cap_sq*). Surprisingly, the thickness of the side wall main beams (*wall_sq*) was the third most important one. A visual inspection of the real bus subject to rollover test confirmed large localized deformations in the cantrail beams. It is clear that the bus columns should be designed as continuous members at the expense of piecewise waistrail and cantrail beams.
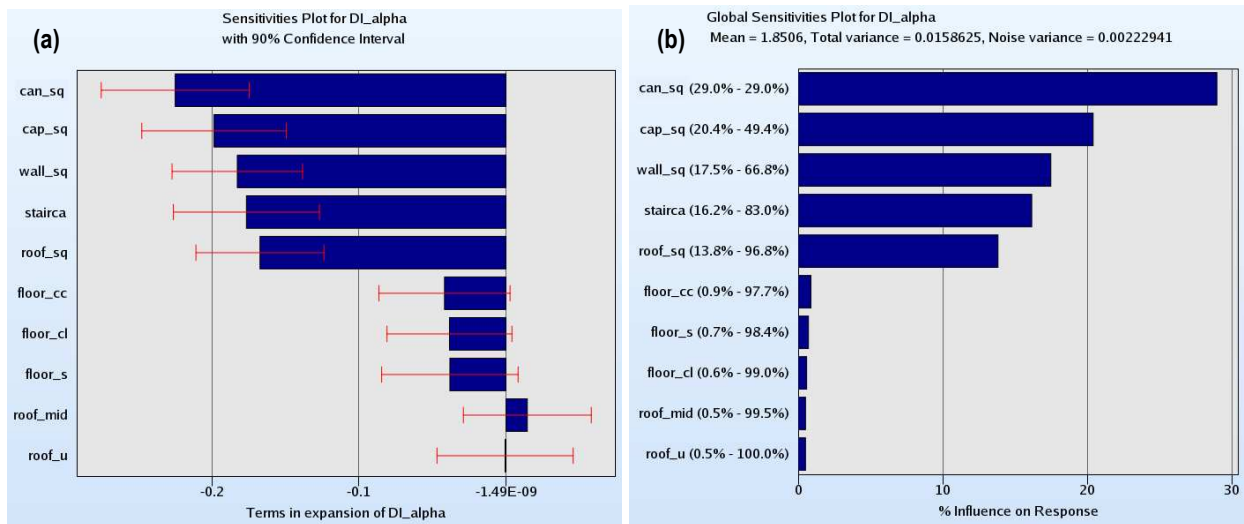

Figure 10: Sensitivity study for response Deformation Index based on (a) ANOVA (b) Sobol's Indices
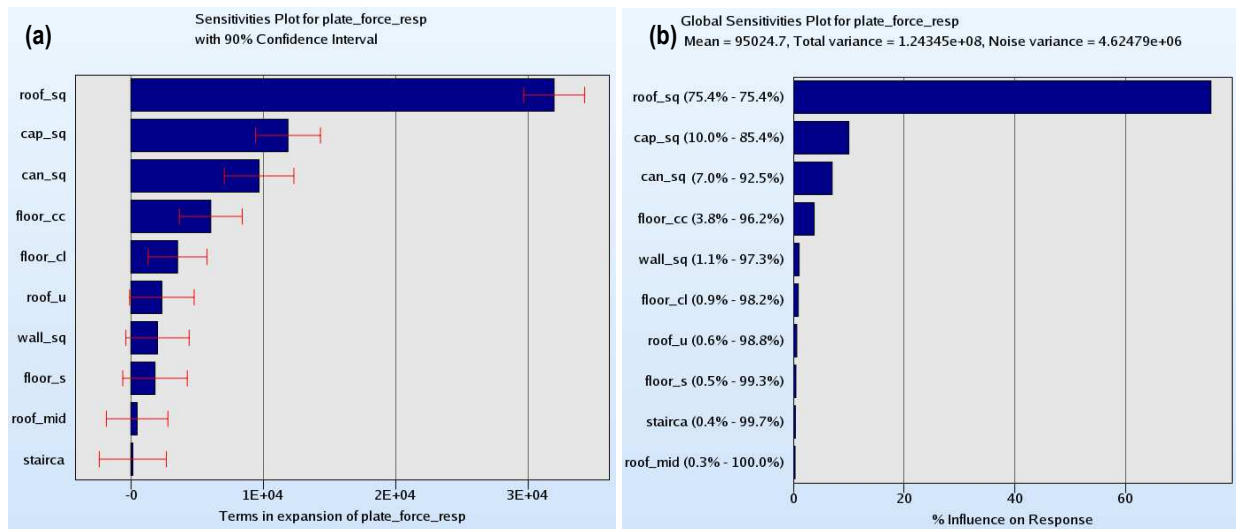

Figure 11: Sensitivity study for response Resultant Force based on (a) ANOVA (b) Sobol's Indices

Figure 11 shows the sensitivity studies for the resultant force in the FMVSS 220 test simulations. Here, as expected, the most important variable was the thickness of the roof bows (*roof_sq*). It was responsible for over 75% of variations in the response function. The other variables are not

as relevant. Figure 12 shows cumulative sensitivity plots for both sets of simulations. The analysis confirms the fact that results of the FMVSS 220 and ECE-R66 tests are divergent. Different elements of the structure influence the response of the bus in each test.
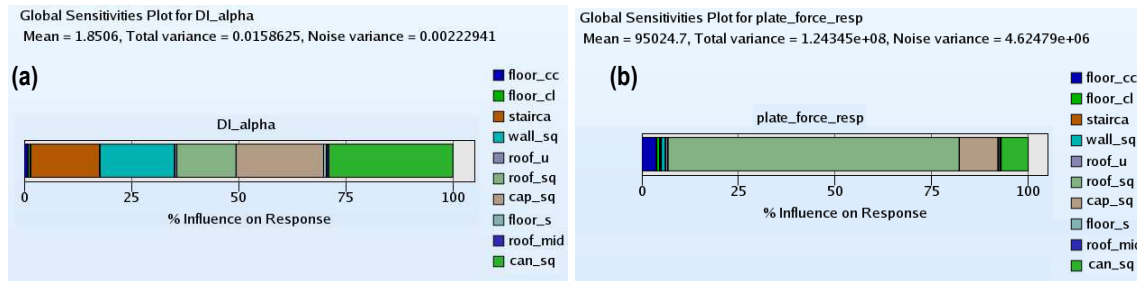

Figure 12: Cumulative global sensitivity in (a) ECE-R66 test (b) FMVSS 220 test

6. Conclusions

This paper presents results of two sets of simulations on dynamic rollover test (according to ECE-R66) and quasi-static roof crush resistance test (according to FMVSS 220). Although both tests are used for the same purpose – assessing the strength of the bus in the approval process - their outcomes diverge. The analyzed bus passes the quasi-static procedure of FMVSS 220 Standard with maximum registered deflection of 119 mm (where 130.2 mm is the limit). However, it considerably fails the dynamic rollover test based per ECE-R66 procedure. The Deformation Index for the structure was noted to be 2.1 (where 1.0 is the limit).

Linear ANOVA and Sobol's Indices were used to identify and rank the most relevant components of the structure in the two tests. As expected the most relevant design variables for the quasi-static load resistance of the roof structure were the roof bows. Variations in this variable were responsible for over 75 % of variations in the plate resistance force. Apparently the same variable was responsible for only ~14 % of variations in the Deformation Index during the rollover test. The connections between the wall and the roof and the front cap structure were found to be the most important at this time.

These results lead to a conclusion that testing paratransit buses according to the FMVSS 220 standard may lead in some cases to erroneous conclusions regarding the bus strength and integrity of its structure.

Acknowledgements

References

(1) United Nations; *Strength of the superstructure of large passenger vehicles. Regulation 66. Revision 1*. http://www.unece.org/trans/main/wp29/wp29regs/r066r1e.pdf, 2006

(2) B. Gepner, et al., *Comparison of ECE-R66 And FMSS 220 Tests for a Selected Paratransit Bus*. TRB 90th Annual Meeting, Paper: 11-1802, 2011

(3) Bojanowski C. Verification, *Validation and Optimization of Finite Element Model of Bus Structure for Rollover Test, Ph.D. dissertation*, Florida State University, May 2009

(4) NCAC, Finite Element Model Archive. 2008, http://www.ncac.gwu.edu/vml/models.html

(5) Kwasniewski L., et al., *Crash and safety assessment program for paratransit buses,* International Journal of Impact Engineering, Pages 235-242, Volume 36, Issue 2, February 2009

(6) Bojanowski C., et al., *Florida Standard for Crashworthiness and Safety Evaluation of Paratransit Buses*, 21st International Technical Conference on the Enhanced Safety of Vehicles, US DOT NHTSA , Paper No. 09-0299-O, Stuttgart, Germany, June 15-18, 2009

(7) Stander N. et al., *LS-OPT® User's Manual - A Design Optimization and Probabilistic Analysis Tool for the Engineering Analyst*, LSTC, Livermore, 2010

(8) Chiu P.W., Bloebaum C.L., *Hyper-Radial Visualization (HRV) Method with Range-Based Preferences for Multi-Objective Decision Making*, Journal of Structural and Multidisciplinary Optimization, Pages 97-115, Volume 40, Numbers 1-6, January, 2010

(9) Archer G.E.B., Saltelli A., Sobol M.I., *Sensitivity Measures, ANOVA-Like Techniques and the Use of Bootstrap*, Journal of Statistical Computation and Simulation, Pages 99 – 120, Volume 58, Issue 2, 1997

APPENDIX A. Gauge conversion to SI and US units

Gauge #	Sheet Steel		Strip and Tubing		Stainless Steel		Galvanized Steel	
	(in)	(mm)	(in)	(mm)	(in)	(mm)	(in)	(mm)
6	0.1943	4.935	0.203	5.156	0.2031	5.159	--	--
7	0.1793	4.554	0.180	4.572	0.1875	4.763	--	--
8	0.1644	4.176	0.165	4.191	0.1719	4.366	--	--
9	0.1495	3.797	0.148	3.759	0.1562	3.967	0.1532	3.891
10	0.1345	3.416	0.134	3.404	0.1406	3.571	0.1382	3.510
11	0.1196	3.038	0.120	3.048	0.1250	3.175	0.1233	3.132
12	0.1046	2.657	0.109	2.769	0.1094	2.779	0.1084	2.753
13	0.0897	2.278	0.095	2.413	0.0937	2.380	0.0934	2.372
14	0.0747	1.897	0.083	2.108	0.0781	1.984	0.0785	1.994
15	0.0673	1.709	0.072	1.829	0.0703	1.786	0.0710	1.803
16	0.0598	1.519	0.065	1.651	0.0625	1.588	0.0635	1.613
17	0.0538	1.367	0.058	1.473	0.0562	1.427	0.0575	1.461
18	0.0478	1.214	0.049	1.245	0.0500	1.270	0.0516	1.311
19	0.0418	1.062	0.042	1.067	0.0437	1.110	0.0456	1.158
20	0.0359	0.912	0.035	0.889	0.0375	0.953	0.0396	1.006
21	0.0329	0.836	0.032	0.813	0.0344	0.874	0.0366	0.930
22	0.0299	0.759	0.028	0.711	0.0312	0.792	0.0336	0.853
23	0.0269	0.683	0.025	0.635	0.0281	0.714	0.0306	0.777